

5G Massive MIMO Antenna Using a Uniform Linear Array: Design, Propagation Standards, Challenges, and Progress

Sakshi Sharma, Roshan Jain

Abstract— Due to the extreme need for bandwidth in the global wireless communication sector, researchers have investigated and studied a wireless access method called massive multiple-input multiple-output (mMIMO) (MIMO). Massively multiplexed antenna systems (MIMO) are a crucial enabling technology for the future generation of networks. By combining antennas at the transmitter and receiver, they provide very efficient use of energy and spectrum with extremely simple processing. To successfully implement 5G networks and beyond, it is essential to understand the massive MIMO system and resolve its core problems. Only then can the intelligent sensing system achieve its many potential benefits. With an emphasis on the existing massive MIMO systems, this study thoroughly investigates the essential enabling technologies needed for 5G networks operating at frequencies below 6 GHz. A multiplexed multiple-input multiple-output antenna system's five most crucial components are covered in this article: gain, isolation, ECC, efficiency, and bandwidth. Two separate types of 5G MIMO antennas for large-scale deployment are described in this article. Use of these types is application-specific and occurs in the sub-6 GHz spectrum. The first kind of massive MIMO antennas were created for use in base stations, however 5G base station antennas using the most recent massive MIMO designs have been introduced. The second kind, designed for mobile devices, compiles findings from studies on various tiny antennas that have been suggested and shown to work with huge MIMO systems. Many people think that mMIMO antennas will be suitable for 5G networks because of this.

Index Terms—5G systems; massive MIMO; base station; smartphone; 5G antennas; 5G applications;

I. INTRODUCTION

The ever-increasing need for faster and more extensive data transfers has wireless communications experts predicting that Fifth Generation (5G) will soon dominate the market. 5G communication networks aim to improve device-to-device connectivity, increase flexibility, and provide larger capacity and data throughput (up to 20 Gbit/s), outstanding reliability, and low latency (1 ms) [1].

The wireless communications industry's global bandwidth crunch prompted the development of massive .. Networks of the future and beyond will rely on this technology. By using arrays of antennas at both the transmitter and receiver ends, multi-user MIMO achieves high spectrum efficiency with little processing requirements and minimal power consumption [2].

Sakshi Sharma, M Tech. Scholar in RCEW, Jaipur
Roshan Jain, Assistant Professor in RCEW, Jaipur

Mobile . technology has greatly advanced the quest for power-efficient, high-quality mobile communication services by reducing transmission power and bandwidth. It may greatly increase data throughput without adding anything else [3]. A large multiple-input multiple-output antenna is fundamental to the design of the 5G communication system. Massive MIMO is an improvement on MIMO that increases throughput and spectral efficiency by using a large number of active communication antennas [5].

The first step in designing a 5G mMIMO system is to determine the kind of element (antenna) and its function. As a result, 5G mMIMO is defined as 5G antennas plus the platform. 5G antennas support MIMO, which stands for multiple-input, multiple-output. They use a myriad of antenna components to simultaneously send and receive large volumes of data. Antennas for mobile apps and 5G base stations must be able to work with many frequencies. You may now get much faster download rates. Furthermore, it enhances the functionality and connectivity of several devices. More data may be sent when the bandwidth is increased. Beamforming, steering, and reception in mobile devices including base stations, smartphones, connected autos, health monitoring equipment, and even industrial machinery rely on antennas such as these [1,6].

Antennas for base stations (BSs) are the fundamental units of every wireless communication network. It might be made up of one or more directional RF antennas that can send and receive radio signals. These base stations, known as antennas, are mounted atop towers and provide cellular coverage to customers. Antennas for multi-band base stations may often be housed in a single radome. One or more base stations, or even certain parts of a single base station, may be linked to each of these antennas via their own unique connectors [7].

Whether the gadget is designed for one user or several users, here is where most of the communication takes place. 5G base stations make use of beam-forming antennas. Additionally, a number of ground targets may be simultaneously focused and steered via a network of antennas [3]. The base station antenna may send signals to a larger number of receivers whether it is located inside or outside. Among the many communications systems that make use of this antenna type are satellite, GPS, GSM, WIMAX, WAN, and LAN networks [8,9].

Devices that need the ability to communicate while in motion greatly benefit from mobile antennas, which provide a variety of advantages. These phones can't support beamforming without multiple-input multiple-output (MIMO) antennas mounted on the exterior and corners. A typical smartphone has around six antennas, two for high- and low-frequency signals. On the other hand, 5G relies on multiple-input

multiple-output (MIMO), which mandates the use of two bands for the bottom band and one band for the upper band. A commonly used combination is 4×2 , or 4T2R.

This implies that the majority of the most recent 5G phones are equipped with four antennas. The capability to autonomously adjust the antenna is likely to be a standard feature of these antennas [13]. The most effective method for preventing interference between mobile phone antennas is to physically separate them. On a little phone, this is quite difficult. Operating frequency, wavelength, and antenna length are all rather high, which is a relief. This is why future phones will have to have additional antennas, especially because the majority of these standards support MIMO antennas [14]. 5G networks that function at frequencies lower than 6 GHz need a wide bandwidth and data transfer rates of 20 Gbps or more.

The 5G bands that were offered include 3.3-4.2 GHz and 4.4-5 GHz, which increases the bandwidth to 100 MHz. In addition to covering large areas, the base station's 3D design incorporates both the azimuth and vertical planes. Antennas for frequencies below 6 GHz should be beefed up in both base stations and phones. 5G networks will have significantly reduced congestion, increased capacity, and improved throughput at higher frequencies because to the increased number of radiating antenna components in a mMIMO array [15]. An ambitious long-term goal is to install a massive sub-6 GHz MIMO array using the radiation aperture of the original 3G, 2G, and 4G antennas [15,16]. In the above use scenarios, the 5G standard enables an uplink data rate that is twice as rapid as the downlink data rate. 5G networks are currently exploring a wide range of technologies. It is believed that the mMIMO system will play a crucial role in directing 5G development. One of the technologies that will support 5G wireless networks is mobile . [19].

A large MIMO system is the outcome of a design in which both the base station and the terminal employ multiple antenna components. Antennas enable several users to communicate at once while making better use of the available spectrum and electricity. With numerous active antennas at the base station, spatial multiplexing makes it possible to communicate with a user endpoint (UE) with the same time-frequency resource [20]. As an added bonus, the beamforming enhancement technique developed for these mMIMO systems may be used to enhance the existing base station hardware with several antennas, cutting down on transmit energy requirements [19,21].

Modern 5G NR networks include state-of-the-art antenna techniques such massive MIMO, which improves data rates (sub-6 GHz), network capacity, coverage, and spectral efficiency. With Massive MIMO, which uses components with multiple antennas, many users may be handled at once [22,23]. Multiplexed MMPO antennas are characterized by their isolation, gain, radiation pattern, phase, and beam width, among other features. If wireless and mobile devices continue to have poor throughput and sluggish data transfer rates, increasing the bandwidth might be a future-proof option [24].

When dealing with space constraints in large-scale arrays, it is necessary to use many solutions that are suitable for the dense capacity of antenna components without increasing the distance between antennas in order to decrease the mutual coupling effects. Due to the high levels of isolation and low correlations brought about by the low levels of reciprocal coupling, the system's performance will not be compromised.

Many decoupling solutions have been suggested, including inserting a metamaterial wall that acts as a spatial band-stop filter or a spatial polarization-rotated wall, and using metal structures between the antenna's components to provide an additional coupling channel [25].

It is challenging to build such decoupling structures in a large-scale MIMO antenna since they all need to be extremely substantial in size. In BSs and smartphone applications, a mutual coupling value of less than -25 dB is ideal, although a value of less than -10 dB is also acceptable. Applying beamforming methods to a mMIMO system has the potential to increase its gain and efficiency. By using several antenna arrays on both the receiving and sending ends of a signal, beamforming is a signal processing method that increases the capacity and performance of a system [26].

Two-Frame Massive MIMO Rectangular planar lattice arrays are among the most basic planar mMIMO architectural designs. A layout of planar arrays with size $N \times M$ is one example [27]. The 2D model element is a widely used component in mMIMO design. A newly constructed dual-band antenna array that shares an aperture and both polarizations might be useful for 5G base stations. The antenna array consisted of a (4×4) planar MIMO array operating in the 3.3-5 GHz band (upper band-UB) and a single antenna element operating in the 0.69-0.96 GHz region (lower band-LB). Built specifically for use in real-world MIMO applications, the UB antenna array is a large rectangular grid array consisting of sixteen antenna components. In order to reduce in-band and cross-band mutual coupling between the UB and LB antennas, Figure shows three decoupling techniques: a ferrite chock ring, a rectangle ring resonator, and a unique baffle design.

Decoupling technology allows for the small combination of the UB and LB antenna arrays, which measure just $0.93 \times 0.93 \times 0.17 \lambda_L$. With HB antennas, a dual-band array can achieve a bandwidth of 41% while with LB antennas, it drops to 32.7%. We provide superior cross-band port isolation of over 30 dB. The UB antenna produces uniform radiation patterns, in contrast to the LB antenna's 8.6 dBi average gain. All operational ranges exhibit radiation efficiency of around 90%. A magneto electric (M.E.) dipole antenna with isolation properties, high gain, and low cross-polarization (X pol) might be created by combining two polarized differential feeding systems. Figure 3b shows the result of designing a modified H-shaped (1-16) differential feed network to feed the 16-antenna array so that it may make advantage of these array properties. By inserting the vertical cross-sections with dotted slots between adjacent dipole units, the array isolation is significantly improved in this case.

A system of high-capacity multi-input multiple-output (MIMO) antennas might be created by disassembling an H-shaped differential power feeding network and its supporting substrate. According to the data, an antenna element operating in the 5G frequency band (i.e., from 3.3 to 5.1 GHz) may achieve a low X-pol of -35.7 dB and a high gain of over 8.1 dBi. The antenna array is well-suited for use in 32-channel capacity MIMO antenna technologies due to its high gain of 17.3 dBi and low envelope correlation coefficient (ECC) value of 0.004 [30,31]. Large, closely spaced antenna arrays that use dual polarization (D.P.) massively multiple-input multiple-output (32T/32R) technology are specifically designed and studied for use in 5G base stations. It is possible to get dual polarization by arranging two aerial

bowtie dipole antennas with chamfers in opposing directions and feeding them with two coaxial cables.

The model incorporates chamfering, which improves isolation to port, and two bowtie aerial arms. Unidirectional radiation is produced when a metal ground plate is positioned at a distance of $\lambda/4$. The radiating component is expected to operate between 3.5 and 4.0 GHz. The simulation results show that the ideal 2-chamfered aerial bowtie dipole antenna with dual polarizations would cover a frequency range of 2.8 to 4.0 GHz, have a gain of 9.1 dBi for both polarizations, a mutual coupling of approximately -25 dB, and an SWR of 1.5. The isolation between the two ports would be -27 dB. The antenna features an easy-to-manufacturable design and a simple overall height of $0.25\lambda_0$ [32,33]. mMIMO antenna system architecture described in detail using patch antennas. Each port in the array has a (2×2) patch antenna sub-array with independent phase stimulation at each element in order to alter the beam's direction and produce lower correlation coefficient values. The array consists of 64 items, or sixteen ports. Its design prioritizes the use of a fixed progressive phase feed network to power the beam-tilts [34].

The following are the parameters of the antenna system: a three-layer FR-4 substrate measuring $33.33 \text{ cm} \times 33.33 \text{ cm} \times 0.16 \text{ cm}$, an operating frequency of 3.6 GHz with a bandwidth of 230 MHz, 5.4 dB gains for each port, and a minimum of 25 dB isolation between neighboring ports [34]. For a large indoor MIMO base station, a portable ultra-wideband MEA was investigated. A key component of the antenna design is the ability of each MEA element to simultaneously activate several characteristic modes.

As shown in Figure 484-port antenna might be constructed using 121 physical antenna components and a (11×11) mMIMO array of $70 \text{ cm} \times 70 \text{ cm}$. The result was a size decrease of 54% compared to the traditional cross-dipole MEA. A reflection coefficient of 10 or less, an intra-element and inter-element connectivity of ≤ -20 at the antenna port, and the ability to operate throughout a broad frequency range of 6 to 8.5 GHz are all characteristics of this antenna. As a whole, the antenna achieves an efficiency of around 70% across all four ports when the 3D radiation patterns are used [35,36]. An Extensive Three-Dimensional ORM The channel characteristics, which might be circular, planar, or cylindrical, are influenced significantly by the layout of the antenna array and, in turn, by the overall performance of the system.

Arrays with circular or flat dimensions often only allow horizontal beam adjustment, which results in a large reduction. We still can't meet the ever-increasing capacity demands with these configurations. One possible remedy to this shortcoming is the use of three-dimensional big array designs such as hexagons, cylinders, triangles, and others [39].

Two models of three-dimensional methods are discussed. The element groupings in the three-dimensional array establish the first kind. An antenna system for 5G base stations was developed employing several array topologies and stacked polyhedral arrays, as shown in Figure, and it operates in the sub-6 GHz range with 1×4 (sector) sub-array configurations. higher than a hundred times higher energy efficiency and ten times more system limit enhancement are possible with a multi-. method. No more than five sectors may be found in any given sector, and each sector has components for a 1×4 sub-array.

On the uppermost layer of each sector are 1×4 patches, with

the bottom and intermediate layers including a distinct ground plane that is in charge of organization. Generally speaking, the system can toggle between two modes: one that just has one port, and another that has a huge MIMO screen and can guide beams. The sub-6 GHz spectrum, which spans from 3.36 GHz to 3.50 GHz, is traversed by the 140 MHz frame's deliberate data transmission. For one sub-array, the dimensions were 280.5 mm in length, 56.1 mm in width, and 2 mm in height. A gain of 12.95 dBi was reached by a single port, whereas a gain of 19.73 dBi was achieved by a single panel with five sectors organized in a rectangular layout. A mutual coupling of around -16 dB was detected in all ports. The radio antenna array system was configured to operate within the frequency range of 3.3 GHz to 3.8 GHz. In order to facilitate 5G, the sub-6 GHz spectrum was globally allocated and concentrated, which is why [20].

Enhanced mobile broadband (eMBB) is one of three possible applications for 5G. Reason being, eMBB employs mMIMO, which stands for multi-antenna maximum-in-space. Below 6 GHz and 28 GHz are two potential 5G frequency ranges. Our goal is to model MIMO antenna systems operating at 26 GHz and 3.5 GHz. There are a total of 108 patches in the antenna described in reference [19]. An array of 96 patches operates at 26 GHz, while 12 patches operate at 3.5 GHz. An internal transmit antenna is what the built antenna will be used for. This antenna is characterized by its connectivity and proximity-coupled feed. According to reference 19, the built antenna has characteristics like a gain of 7.3 dB, an s-parameter result of around -10.8199 dB, and a mutual coupling of approximately -32.6201 dB.

The more components a mMIMO system has, the larger its channel capacity will be. The majority of previous studies have investigated the ideal number of antennas to get a certain gain, supposing that each antenna in a large array has the same gain. The bulk of these studies have concentrated on channel properties, examining how edge effects and mutual coupling affect the gain variation in large-scale MIMO arrays of 32 elements.

Current high-volume MIMO experiments mostly employ patch and dipole antennas, which were the primary focus of the impact research. Compared to dipole arrays, finite patch arrays have less gain pattern variation. Because there is a lot of diversity in the gain patterns, not every antenna in the huge MIMO system helps out every user, and it becomes worse when it comes to detecting how many effective antennas a single user has. A 20% delay for patch arrays and a 35% slowdown for dipole arrays are encountered by the zero-force MIMO detector for all users, according to the findings obtained at the system level. However, user unfairness and inequity result from mixing maximal ratios. A huge MIMO test bench in an anechoic chamber allows for measurements to be taken from each of the 32 active components of an antenna array, which is crucial for precise antenna measurements.

When looking to boost system throughput, patch arrays are your best bet. The microstrip variant's 31 mm square patch was formed by two 1.4 mm wide U-slots that merged into one another. Next, we moved on to the 3.4–3.6 GHz and 2.4–2.62 GHz bands. We did most of our comparing at 2.6 GHz. A limited number of antenna components showed a broad diversity of gain patterns, according to the experiments. We get this angle-dependent beamforming as a result of mutual coupling and the edge effect. Because of the stronger

mutual coupling in a dipole array, the gain variation is larger. Thus, an omni-directional array will exhibit more angle sensitivity as contrasted with a directional patch array [10]. The eigenvalue distribution and two-user MU-MIMO (multi-user MIMO) capacity were investigated within a realistic urban macro (UMa) setting operating at 3.5 GHz utilizing a zero-forcing block diagonalized (ZFBD) method. Having twenty-four Tx components rather of eight was discussed. When the numbers expanded rapidly, there was almost no improvement compared to independent channels with the same distribution (i. i. d.). Nevertheless, ratios of 63% and 73% were achieved for Tx numbers up to 64 and 128 respectively. Although it was still small, the trend toward eigenvalue homogeneity became more noticeable as Tx increased.

Still present in the observed environment are (i. i. d.) channel gaps, despite the fact that mMIMO produces more ordered sub-channels and de-correlated user channels compared to normal MIMO. Antenna arrangement affects receive and transmit performance, and increasing the number of antennas installed per user improves capacity. Consequently, orthogonal user channel representation is not used in the measurement procedure [11,12].

The ability of massive MIMO to make full use of existing space resources, greatly improve spectrum efficiency, and resolve the present spectrum resource issue makes it stand out among the technologies being explored for 5G mobile communication systems. Documenting the present MIMO setup's radio channel characteristics is essential for studying mMIMO technology.

Using a massive 64-component virtual antenna array, an outside 3.33 GHz measurement experiment was conducted. It seems from the data that the most common channel parameters, such as the power delay profile (PDP), azimuth spread (AS), and delay spread (OS), displayed the predicted behavior. Channel dynamics are shown by data from the spatial and latency domains for large arrays. Results may inform models of 5G communication systems and massively multi-input multiple-output (mMIMO) channels [13,14].

An inexpensive 16-port MIMO non-planar antenna system was built using a 3D octagonal polystyrene block for usage in future 5G applications. The octagonal polystyrene block's bottom and top could be seen thanks to the MIMO pieces arranged on all eight sides. A slotted microstrip patch, a broken ground plane, and a step-biased feed line were all parts of the antenna. The 22 mm x 20 mm FR4 substrate was used to build each MIMO element for 5G applications. These elements operate in the 3.35-3.65 GHz frequency range. To enhance the isolation between the array components, a negative-sign exponential metamaterial decoupling structure (NZI-ENG) was used. Array components were placed on top of the ground planes and isolation structures for common connections, which were positioned in the bottom layer [15]. With the help of the metamaterial-based decoupling structure, the antenna components may be arranged side by side with a separation of more than 28 dB.

All of the metrics were within the acceptable range, with total active reflection coefficient (TARC) values below -18 dB, channel capacity loss (CCL) values below 0.30, and an envelope correlation coefficient (ECC) below 0.10. When several 5G devices are wirelessly linked to a central server, the proposed non-planar 3D-MIMO antenna technology might be useful for indoor positioning systems and wireless

personal area networks [16]. A high number of antennas at the transmitter and receiver ends allow most 5G MIMO systems to accomplish spatial multiplexing. This proposed 16-element indoor BS antenna array may operate in the 3.3-6.0 GHz range and was developed with 5G in mind.

Bands 42/43/46-N77-N78-N79, which are part of the LTE network, were covered by a monopole antenna. Adjacent to it on a base was an antenna component, a printed hexa-kaidecagon polygon. After positioning the antenna components to provide superior polarization diversity and isolation, the projected BS array was developed, built, and evaluated by examining radiation patterns, S-parameters, overall results, and antenna performance. Findings and model

In this work, we study ULA radiation and reception patterns and use an angular domain model of the MIMO channel. The total is comprised of the two sub-projects MASO (multiple input, single output) and SIMO (single input, multiple output). Furthermore, the following input parameters must be supplied.

Details of the inputs:

- "N" represents the overall count of antennas.
- The normalized antenna separation Δ (normalized to the wavelength)
- The intended signal's radiation or reception directions
- The interfering signal's radiation or reception directions

Here are the results:

How signals received in different directions are related to one another

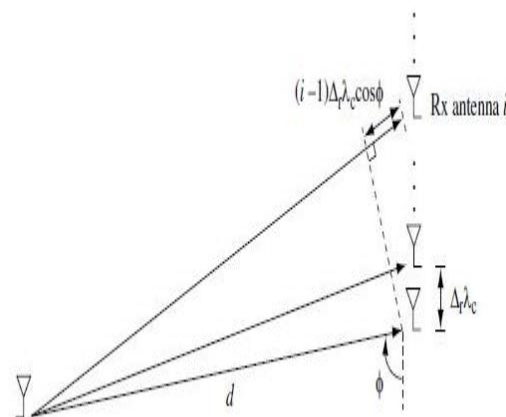
Think about the signal-to-noise ratio (SINR) of several input signals (different receiving directions) with diversity combining, the ULA's polar beamforming pattern, and signal-to-interference ratio (fading) for signals and interference.

Computer program

The time-invariant channel is defined by the equation $y = Hx + w$, which includes the sent signal x , the received signal y , and white Gaussian noise w . Both the SIMO and MISO LOS (Line-of-Sight) channels are shown in the two pictures that follow. A single axis defines the consistent spacing of antennas in a linear array.

The SIMO model's LOS

Here is a picture of the SIMO model:



Channel gain:

$$\mathbf{h} = [h_1, \dots, h_{n_r}]^T = a \cdot \exp\left(\frac{j2\pi d}{\lambda_c}\right) \begin{bmatrix} 1 \\ \exp(-j2\pi\Delta_r\Omega) \\ \vdots \\ \exp(-j2\pi(n_r - 1)\Delta_r\Omega) \end{bmatrix}$$

a: path attenuation, which is assumed to be constant across all possible antenna pairings Due to the fact that the distance between antennas is substantially less than that between the transmitter and receiver, the distance between each antenna pair may be expressed as:

$$d \approx d + (i - 1)\Delta_r$$

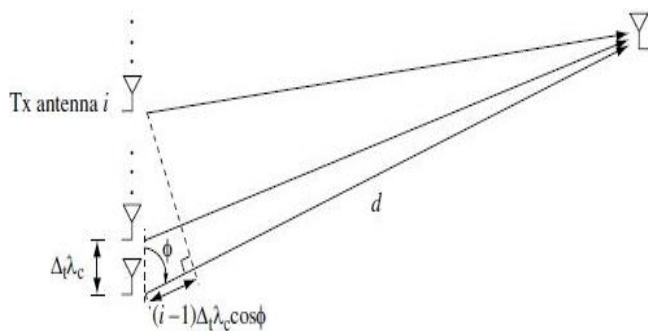
$$\cos \phi,$$

$$i = 1, \dots, n_r$$

Directional cosine is defined as $\Omega = \cos \phi$. The gain of the channel will be:

Death of the MISO Model

The MISO model is shown in the following image:



Similar to SIMO model, the channel gain is:

$$\mathbf{h} = [h_1, \dots, h_{n_t}]^T = a \cdot \exp\left(\frac{j2\pi d}{\lambda_c}\right) \begin{bmatrix} 1 \\ \exp(-j2\pi\Delta_t\Omega) \\ \vdots \\ \exp(-j2\pi(n_t - 1)\Delta_t\Omega) \end{bmatrix}$$

Signals may be represented in the angular domain. Each linear transformation may be written as the combination of three distinct operations—a rotation, a scaling, and a second rotation. It is possible to do an SVD on H: U and V are (rotation) unitary matrices; Λ is a rectangular matrix; and $H = U\Lambda V^*$

SIMO

Specified inputs:

- $N_r = 5$ indicates a total of 5 receiving antennas.
- Antenna spacing, normalized to a value of 1/2
- The preferred signal's directional reception: $\pi/4$
- The interference signal's directional reception: $\pi/2$
- Connection between signals coming from opposite directions of transmission or reception To visualize the relationship between two signals, we utilize the expression

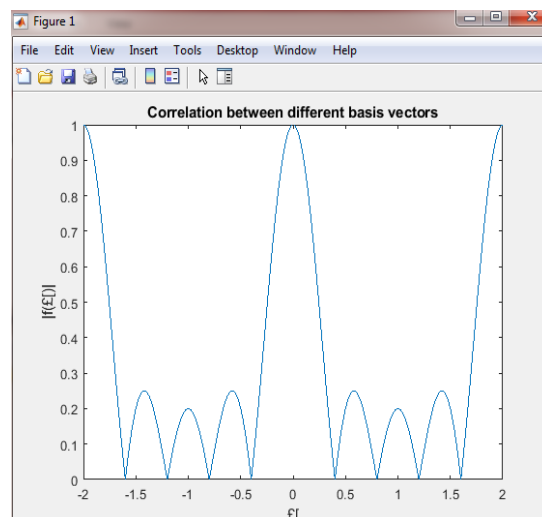


Figure 1: Correlation between different basis vectors

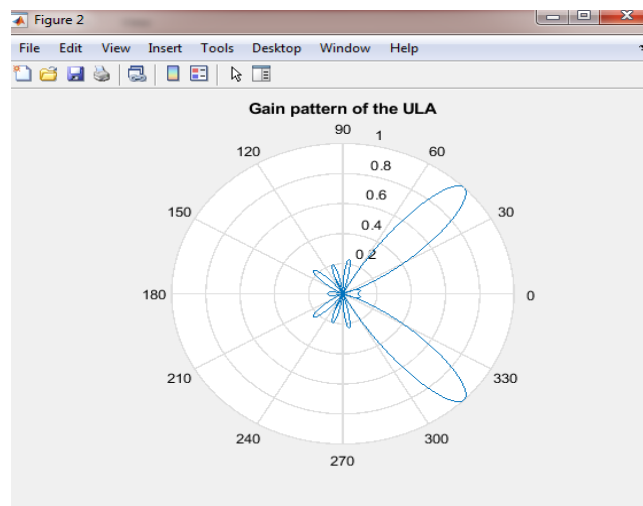


Figure 2 Gain Pattern of ULA

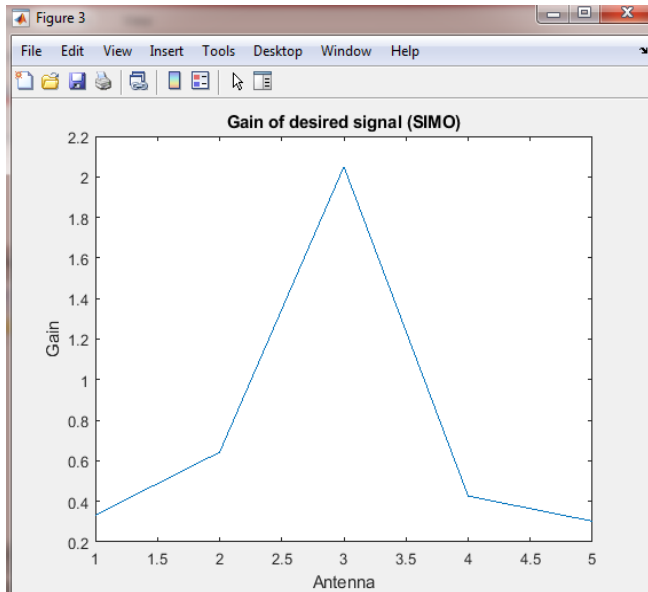


Figure 3 :- Gain of desired signal

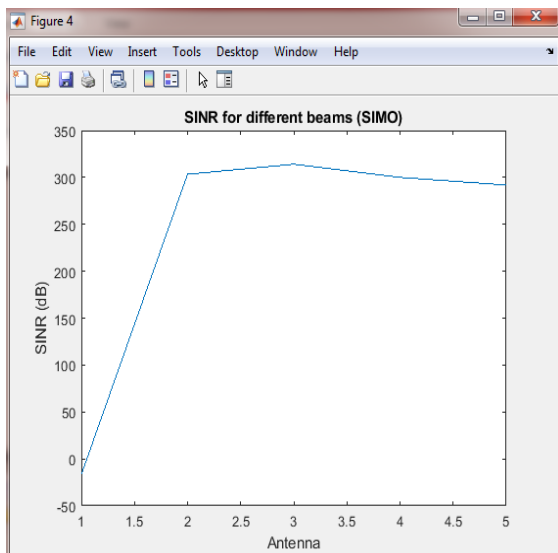


Figure 4:- SINR for different beams (SIMO)

Figure 5:- SINR for angle beams (SIMO)

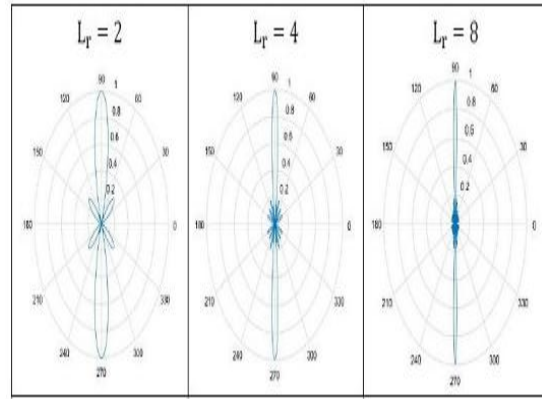


Figure 6:- SINR for angle beams (SIMO)

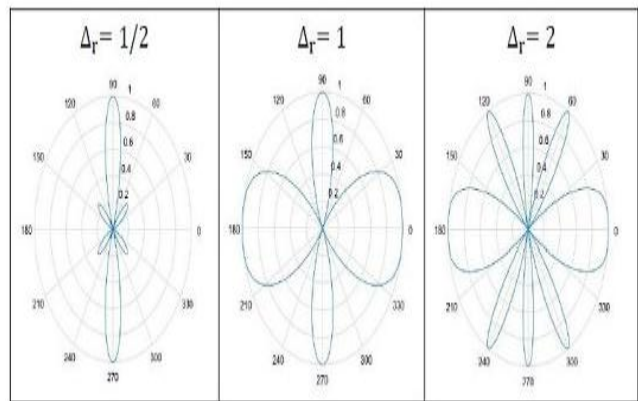


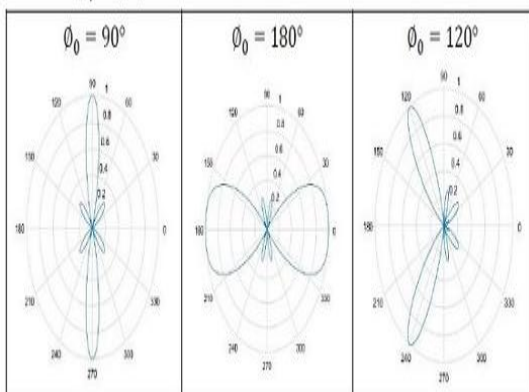
Figure 7:- SINR for angle beams (SIMO)

With diversity combining, the signal-to-noise ratio (SNR) of various input signals (multiple receiving directions) improves. Using MRC (Maximal ratio combining), I executed this section, and the resulting SINR was 16.9243 dB.

MISO

Specified inputs:

- $N_t = 7$ = Number of antennas used for receiving
 - Antenna spacing, normalized to a value of 1/2
 - Preferred signal reception azimuths: /6
 - The axis along which the interference signal is received: /3
- MISO yields essentially the same effect as SIMO.



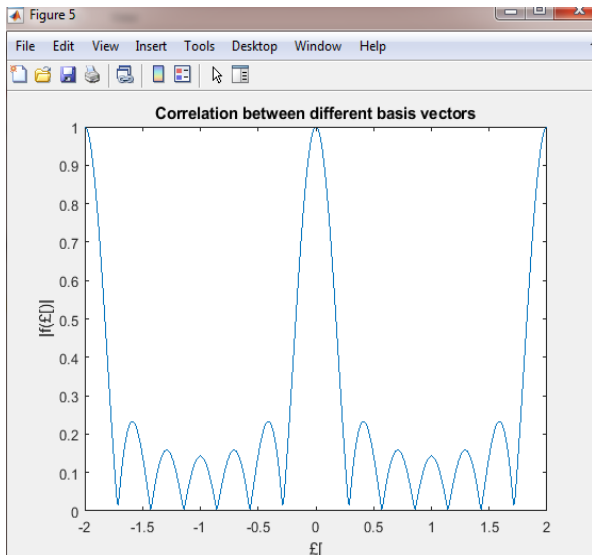
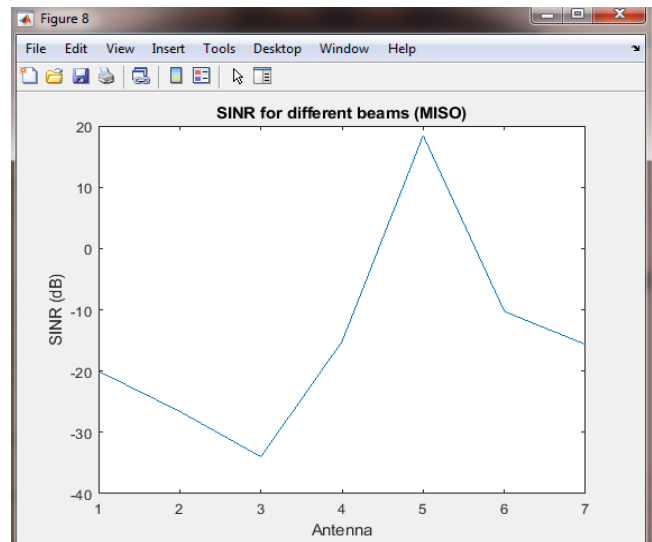


Figure 8 :- Correlation between different basis vectors



With diversity combining, the signal-to-noise ratio (SNR) of various input signals (multiple receiving directions) improves. I have mixed several broadcast signals as though they were received. When I use the MRC technique, I get a SINR of 35.75 dB.

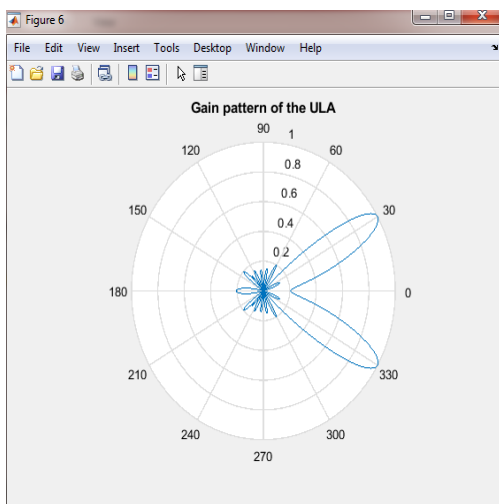
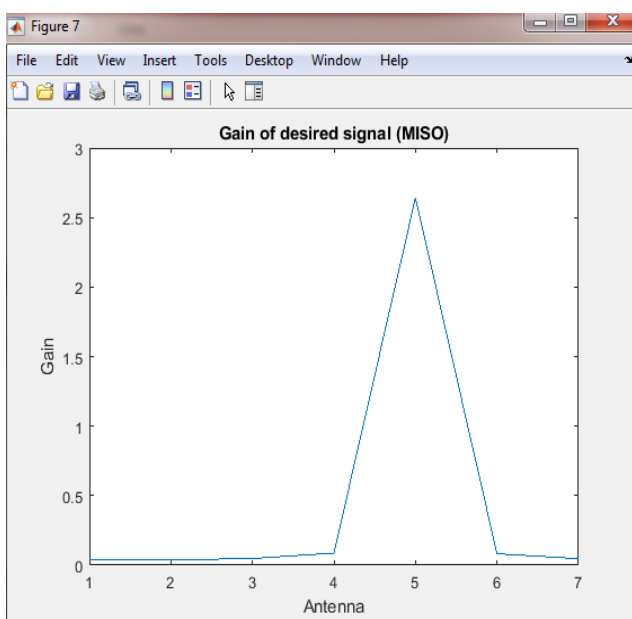


Figure 9:-Gain pattern



5. Conclusions

The 5G infrastructure relies heavily on massive MIMO. A plethora of antennas, on the part of both base stations and mobile devices, are used by 5G massive MIMO. A huge MIMO system's performance is improved by increasing the number of base station antennas in accordance to the number of users and devices. Antennas' spatial correlation and mutual coupling are both important factors. 5G antennas will need special properties for massive MIMO to function in both cases. Consequently, the growth characteristics of massive MIMO systems that are applicable to both ways may be satisfied by a large number of 5G antennas. While smartphones are limited to 20 antenna elements, 5G mid-band base stations with large MIMO antenna systems may accommodate up to 256 elements for sub-6 GHz frequencies.

REFERENCES

- [1] Pant, M.; Malviya, L. Design, developments, and applications of 5G antennas: A review. *Int. J. Microw. Wirel. Technol.* **2022**, 1–27. [[Google Scholar](#)] [[CrossRef](#)]
- [2] Jain, A.; Yadav, S.K. Design and analysis of compact 108 element multimode antenna array for massive MIMO base station. *Prog. Electromagn. Res. C* **2016**, 61, 179–184. [[Google Scholar](#)] [[CrossRef](#)] [[Green Version](#)]
- [3] Rahayu, Y.; Sari, I.; Ramadhan, D.; Ngah, R. High gain 5G MIMO antenna for mobile base station. *Int. J. Electr. Comput. Eng.* **2019**, 9, 468. [[Google Scholar](#)] [[CrossRef](#)]
- [4] Kumar, S.; Dixit, A.; Malekar, R.; Raut, H.; Shevada, L.K. Fifth generation antennas: A comprehensive review of design and performance enhancement techniques. *IEEE Access* **2020**, 8, 163568–163593. [[Google Scholar](#)] [[CrossRef](#)]
- [5] Borges, D.; Montezuma, P.; Dinis, R.; Beko, M. Massive mimo techniques for 5g and beyond—Opportunities and challenges. *Electronics* **2021**, 10, 1667. [[Google Scholar](#)] [[CrossRef](#)]
- [6] Ikram, M.; Sultan, K.; Lateef, M.; Alqadami, A.S.M. A Road towards 6G Communication—A Review of 5G Antennas, Arrays, and Wearable Devices. *Electronics* **2022**, 11, 169. [[Google Scholar](#)] [[CrossRef](#)]

- [7] Farasat, M.; Thalakatuna, D.; Hu, Z.; Yang, Y. A review on 5G sub-6 GHz base station antenna design challenges. *Electronics* **2021**, *10*, 2000. [[Google Scholar](#)] [[CrossRef](#)]
- [8] Azim, R.; Siddique, A.K.M.A.H. Ground Defected Planar Super-wideband Antenna: A Suitable Transceiver for Short Distance Wireless Communication. *J. Kejuruter.* **2018**, *30*, 129–139. [[Google Scholar](#)] [[CrossRef](#)]
- [9] Olokede, S.S.; Ain, M.; Othman, M.; Ullah, U.; Ahmad, Z.A. Design of Microstrip Line-Coupled Isosceles-Triangular Loop Resonator Antenna. *J. Kejuruter.* **2013**, *25*, 39–45. [[Google Scholar](#)] [[CrossRef](#)]
- [10] Salleh, A.; Chiou, C.; Alam, T.; Singh, M.; Singh, J.; Tariqul, M. Development of Microwave Brain Stroke Imaging System using Multiple Antipodal Vivaldi Antennas Based on Raspberry Pi Technology. *J. Kejuruter.* **2020**, *32*, 39–49. [[Google Scholar](#)]
- [11] Corak, P.; Antena, S.; Tali, T.; Radar, A.; Tanah, P. Radiation Pattern Performance of Bow Tie Patch Antenna for Ground Penetrating Radar (GPR) Applications. *J. Kejuruter.* **2021**, *4*, 153–160. [[Google Scholar](#)]
- [12] Jainal, S.F. Ultra-Wideband Planar Antenna with Notched-Band for WIMAX, WLAN and MSAT Applications. *J. Kejuruter.* **2020**, *32*, 455–465. [[Google Scholar](#)]
- [13] Khan, R.; Al-Hadi, A.; Soh, P.; Kamarudin, M.; Ali, M.; Owais. User influence on mobile terminal antennas: A review of challenges and potential solution for 5G antennas. *IEEE Access* **2018**, *6*, 77695–77715. [[Google Scholar](#)] [[CrossRef](#)]
- [14] Anguera, J.; Andújar, A.; Huynh, M.; Orlenius, C.; Picher, C.; Puente, C. Advances in antenna technology for wireless handheld devices. *Int. J. Antennas Propag.* **2013**, *2013*, 838364. [[Google Scholar](#)] [[CrossRef](#)] [[Green Version](#)]
- [15] Rahman, M.M.; Islam, M.S.; Islam, M.T.; Al-Bawri, S.S.; Yong, W.H. Metamaterial-Based Compact Antenna with Defected Ground Structure for 5G and Beyond. *Comput. Mater. Contin.* **2022**, *72*, 2383–2399. [[Google Scholar](#)]
- [16] Marcus, M.J. Spectrum policy and regulatory issues. *IEEE Wirel. Commun.* **2019**, *26*, 9. [[Google Scholar](#)] [[CrossRef](#)]
- [17] Behta, K.; Ziolkowski, C.; Kelner, J.; Nowosielski, L. Modeling of downlink interference in massive mimo 5g macro-cell. *Sensors* **2021**, *21*, 1–17. [[Google Scholar](#)] [[CrossRef](#)]
- [18] Zeydan, E.; Dedeoglu, O.; Turk, Y. Experimental Evaluations of TDD-Based Massive MIMO Deployment for Mobile Network Operators. *IEEE Access* **2020**, *8*, 33202–33214. [[Google Scholar](#)] [[CrossRef](#)]